ORIGINAL ARTICLE

Cone-beam CT radiomics features might improve the prediction of lung toxicity after SBRT in stage I NSCLC patients

Qingjin Qin[1,2†] (iD), Anhui Shi[3,4†], Ran Zhang[2,5] (iD), Qiang Wen[6], Tianye Niu[7], Jinhu Chen[2], Qingtao Qiu[2], Yidong Wan[8], Xiaorong Sun[1,5,9] & Ligang Xing[1,2]

1 School of Medicine and Life Sciences, University of Jinan-Shandong Academy of Medical Sciences, Jinan, China
2 Department of Radiation Oncology, Shandong Cancer Hospital and Institute, Shandong First Medical University and Shandong Academy of Medical Science, Jinan, China
3 Key Laboratory of Carcinogenesis and Translational Research (Ministry of Education), Beijing, China
4 Department of Radiation Oncology, Peking University Cancer Hospital & Institute, Beijing, China
5 Shandong University Cheeloo College of Medicine, Jinan, China
6 Department of Oncology, Shandong Provincial Hospital, Shandong Provincial Hospital Affiliated to Shandong University, Jinan, China
7 Nuclear & Radiological Engineering and Medical Physics Programs Woodruff School of Mechanical Engineering Georgia Institute of Technology, Atlanta, Georgia
8 Institute of Translational Medicine, Zhejiang University, Hangzhou, Zhejiang
9 Department of Nuclear Medicine, Shandong Cancer Hospital and Institute, Shandong First Medical University and Shandong Academy of Medical Science, Jinan, China

Abstract

Background: Stereotactic body radiotherapy (SBRT) is the standard care for inoperable early stage non-small cell lung cancer (NSCLC). The purpose of our study was to investigate whether a prediction model based on cone-beam CT (CBCT) plus pretreatment CT radiomics features could improve the prediction of tumor control and lung toxicity after SBRT in comparison to a model based on pretreatment CT radiomics features alone.

Methods: A total of 34 cases of stage I NSCLC patients who received SBRT were included in the study. The pretreatment planning CT and serial CBCT radiomics features were analyzed using the imaging biomarker explorer (IBEX) software platform. Multivariate logistic regression was conducted for the association between progression-free survival (PFS), lung toxicity and features. The predictive capabilities of the models based on CBCT and CT features were compared using receiver operating characteristic (ROC) curves.

Results: Five CBCT features and two planning CT features were correlated with disease progression. Six CBCT features and two planning CT features were related to lung injury. The ROC curves indicated that the model based on the CBCT plus planning CT features might be better than the model based on the planning CT features in predicting lung injury. The other ROC curves indicated that the model based on the planning CT features was similar to the model based on the CBCT plus planning CT features in predicting disease progression.

Conclusions: Both pretreatment CT and CBCT radiomics features could predict disease progression and lung injury. A model with CBCT plus pretreatment CT radiomics features might improve the prediction of lung toxicity in comparison with a model with pretreatment CT features alone.

Key points

- **Significant findings of the study**: A model with cone-beam CT radiomics features plus pre-treatment CT radiomics features might improve the prediction of lung toxicity after SBRT in stage I NSCLC patients.
- **What this study adds**: In the prediction of PFS and lung toxicity in early-stage NSCLC patients treated with SBRT, CBCT radiomics could be another effective method.

Introduction

Stereotactic body radiotherapy (SBRT) uses modern radiation technologies and high conformal radiation treatment planning to deliver high radiation doses to restricted volumes through multiple precisely aimed radiotherapy beams, which maximizes the dose within the target volume and minimizes the dose to the surrounding organs at risk (OARs).[1–3] SBRT is a guideline-recommended treatment choice for patients with early-stage non-small cell lung cancer (NSCLC) who are not surgical candidates or do not accept the risk of surgery.[4] Most phase I and II trials have confirmed the feasibility, safety, and efficacy of SBRT with excellent local control and quality of life. Several retrospective studies and prospective trials have also reported that the survival outcomes after SBRT were comparable with those after surgical resection.[5–9] The phase III randomized trial (CHISEL) of SBRT versus conventional radiotherapy for stage I inoperable NSCLC demonstrated that the two-year local control (LC) and overall survival (OS) rates improved from 65% and 59% in standard radiotherapy to 89% and 77% in SBRT, respectively.[10]

Moreover, investigations have found that a proportion of patients would develop local failure (9%), regional lymph node metastases (1%) or more distant metastasis (9%) after SBRT.[10] Therefore, improved disease outcomes and reduced chances of lung injury can be achieved with individualized treatment.[11–13] In recent years, medical imaging as a way to predict clinical outcomes and lung injury has become a cornerstone of personalized cancer. Novel advanced imaging analysis techniques, including radiomics to extract quantitative features from medical images such as computed tomography (CT) and positron emission tomography (PET), can identify a patient's response to treatment or the probability of developing side effects.[11,14–20] However, the role of pretreatment CT radiomics features in predicting tumor control or lung injury still warrants validation by summarizing previous research.[18–20]

In addition to baseline PET or CT images, cone-beam CT (CBCT) images can provide very useful information for tumor control and/or toxicity. Three-dimensional (3D) cone-beam CT (CBCT) images are routinely acquired

during SBRT in NSCLC for patient setup and positioning verification.[21] These images can provide data on the day-to-day changes of the tumor and normal tissue during the course of irradiation.[22] Previous studies have shown that tumor volume reduction and CT number changes in CBCT images could potentially predict the treatment response for lung cancer.[23–25] However, these findings were inconsistent and inconclusive. In the present study, we analyzed the radiomics features of pretreatment CT and series of CBCT images. The aim of the study was to investigate whether a model that combined cone-beam CT (CBCT) with pre-treatment CT radiomics features could better predict tumor control and lung toxicity after SBRT than a model with pre-treatment CT features alone.

Methods

Patient selection

Patients with stage I NSCLC treated with SBRT from July 2016 to April 2018 at the Shandong Cancer Hospital were retrospectively included. The inclusion criteria were as follows: primary NSCLC confirmed by biopsy, TNM stage I (AJCC version 7), and treatment with SBRT. The exclusion criteria were previous lung radiation, more than one lung tumor or other concurrent tumors and lack of follow-up data. The clinical information included sex, age, pathology, clinical stage information, smoking history, radiation treatment planning, treatment response and lung injury data collected from the electronic medical records. The study was approved by the Research Ethics Committee of Shandong Cancer Hospital. All the protocols and methods were in accordance with the guidelines and regulations. Informed consent was provided by all participants.

SBRT simulation, planning and treatment

All patients were immobilized in a customized mold in the supine position with their arms raised above their heads for simulation in the CT simulator (Philips Big-bore brilliance CT). Briefly, the patients were immobilized on a

Table 1 Clinical characteristics

Clinical features	*n*	%
Gender		
Female	8	23.5
Male	26	77.5
Age, median (range) (years)		
69 (50–84)		
Age		
≤ 65	12	35.3
65–80	17	50
≥ 81	5	14.7
Pathological type		
Adenocarcinoma	19	55.9
Squamous cell carcinoma	9	26.5
Other	6	17.6
T stage		
T1	22	64.7
T2	12	35.3
Smoker		
No	11	32.4
Yes	23	67.6
Biological effective dose		
<100 Gy	8	23.5
100–120 Gy	26	76.5

vacuum couch, and a free-breathing simulation CT (such as 4D-CT) was performed. Abdominal compression was utilized if the tumor motion was greater than 1 cm. Cone-beam CT and portal imaging combined with a linear accelerator were used for daily setup and image-guided treatment. The gross tumor volume (GTV) was delineated in the lung window, and an internal target volume (ITV) was generated in light of the breathing form of the patient. Finally, an isotropic margin of 5 mm axially and 1 cm craniocaudally was added to generate the planning target volume (PTV) with no clinical target volume (CTV) margin. The designed and normalized radiotherapy plans were generated on the Varian treatment planning system (Eclipse version 13.6, Varian, USA). To calculate the biological effective dose (BED), the value of α/β was defined as 10. As shown in Table 1, 76.5% of the BED for radiation treatment in our study was concentrated in the range of 100–120 Gy.

Planning CT and CBCT image analysis

As a part of the SBRT course, planning CT images were obtained from the SBRT simulation, and chest CBCT images were obtained prior to each radiation delivery. All CBCT images were acquired using the thoracic imaging protocol on a Varian Linac CBCT with a voltage of 110 kV, tube current of 20 mA, and exposure time (total pulsed beam-on time) of 7–14 seconds. The detector size was 25 cm × 25 cm, and the source to detector distance was 150 cm. The 2.5 mm contiguous axial images were transferred to the Varian workstation, and the view was reconstructed into a 250 × 250 × 200 mm field. Each serial CBCT image used Monte Carlo-based scatter correction and ring artifact correction.[26,27] A radiation oncologist (XLG, with 20 years of experience) manually contoured the region of interest (ROI) using the open-source imaging biomarker explorer (IBEX) software (http://bit.ly/IBEX_MDAnderson). All the planning CT and CBCT images were set to a window/level of 600/1000 HU to contour the ROI (Fig 1) of the primary tumor, and the radiomics features were analyzed using IBEX. A total of 187 radiomics features were initially selected automatically, including the Gray Level Co-occurrence Matrix, Gray Level Run Length Matrix, Intensity Direct, Neighbor Intensity Difference and Shape. The features calculation was performed using IBEX.

Patient follow-up and outcomes

The patients were followed-up with clinical examinations and chest CT imaging in the first month, every three months in the first year, and every six months in the second year after the treatment, and annually thereafter. Suspicious findings were further evaluated with bone scintigraphy or brain magnetic resonance (MR) imaging, PET scans, biopsy, or other methods.

Radiation pneumonitis was graded according to the Common Terminology Criteria for Adverse Events (CTCAE) version 4.0. Disease progression was based on the RECIST systems. The form of disease progression, including local failure (LF), nodal failure (NF), and distant failure (DF), was determined by reviewing all imaging studies and clinical information. Progression was confirmed by biopsy, PET/CT, or CT images at follow-up. The above data were recorded as the date of the first CT or PET/CT scan.

Statistics analysis

All statistical analyses were performed using the Statistical Package for Social Sciences software (SPSS v20; Chicago, IL, USA) and MedCalc 19.0. At first, 187 radiomics features were automatically selected for each CBCT or planning CT image. The CBCT images of each patient included the first CBCT (CBCT1), intermediate CBCT (CBCTmid), and last CBCT (CBCTlast) during SBRT. A total of 144 radiomics features of each CBCT or planning CT image were used to conduct a multivariate logistic regression after deleting the missing and identical radiomics features. The missing radiomics features were supplemented using the multiple interpolation method. The radiomics features were selected using the forward stepwise selection method. Finally, the effective radiomics features of the

Figure 1 Region of interest (ROI) on the (**a**) planning CT (**b**) CBCT1 (**c**) CBCTmid and (**d**) CBCTlast for a representative case.
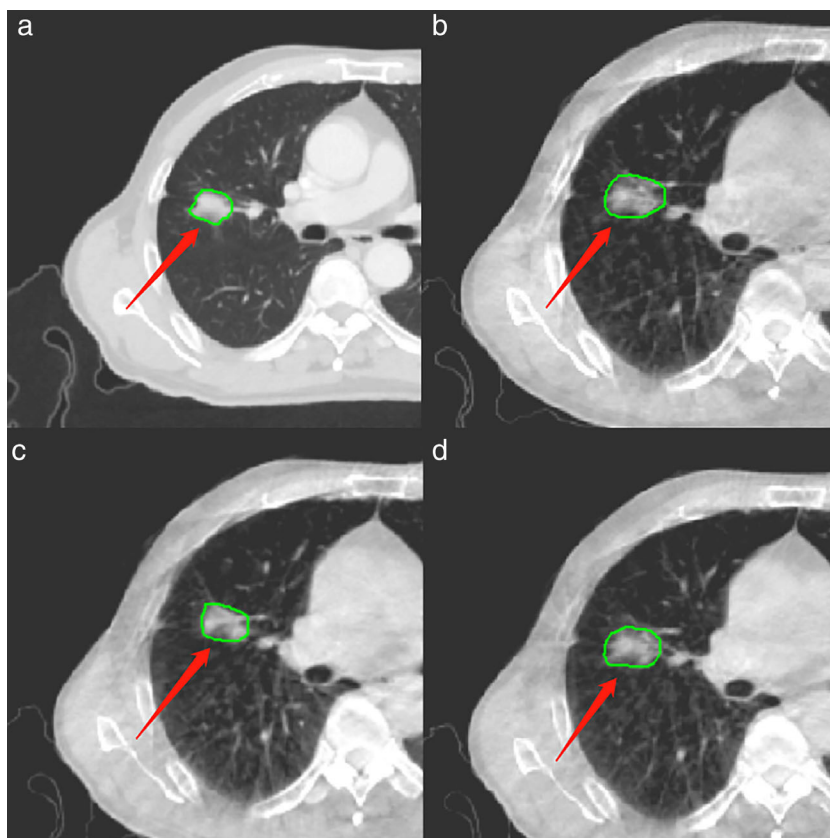
CBCT and planning CT images were associated with the progression and lung injury of early-stage NSCLC patients treated with SBRT. Comparisons of different prediction models based on CBCT and CT radiomics features were conducted with ROC curves. DeLong's test was used for difference in area under the curve (AUC).[28]

Results

Patient characteristics and clinical outcomes

The demographic information is provided in Table 1. A total of 34 patients were enrolled, including 26 males and eight females, with an average age of 69 years (58–84 years). Pathological types were classified as adenocarcinoma (55.9%), squamous cell carcinoma (26.5%) and other types (17.6%). All patients had stage I NSCLC, including T1 stage (64.7%) and T2 stage (35.3%) disease.

The median follow-up time was 20 months. A total of 5.9% patients had local failure alone (*n* = 2), 2.9% had mediastinal lymph node metastasis alone (*n* = 1), 8.8% had both lymph node and distant metastases (*n* = 3), and 5.9% had distant failure only (*n* = 2). A total of 23.5% of patients (*n* = 8) experienced lung injury, with 17.6% being grades 1 and 2 (*n* = 6) and 5.9% being grade 3 (*n* = 2).

Correlation between radiomics features analysis and PFS

Two planning CT radiomics features (GLCM3: Variance and ID: Global Media) were significantly correlated with progression. With each unit increase of the index (GLCM3: Variance and ID: Global Media), the risk of disease progression increased 8.580 (OR = Exp [B] = 9.58) and 50.8% (OR = Exp [B] = 1.508) times, respectively. AUC was 0.894, and the 95% CI was 0.766–1.000 (Table 2).

Three radiomics features (GLCM3: Cluster Shade, ID: LocalEntropyMax and SHAPE: Orientation) of CBCT1 were significantly correlated with disease progression. With each unit increase of the index GLCM3: Cluster Shade, the risk of disease progression increased 1.778 times (OR = Exp [B] = 2.778); with each unit increase of the index ID: Localtropy Max, the risk of disease progression decreased (OR = Exp [B] = 0.000); with each unit increase of the index SHAPE: Orientation, the risk of disease progression decreased (OR = Exp [B] = 0.943); and with each unit decrease of the index (SHAPE: Orientation, the risk of disease progression was 1.06 times lower (OR = Exp

Table 2 The radiomic features correlated with disease progression

| Radiomic features | P-value | Exp (B) | Exp (B) 95% CI | | Logistic regression AUC (95%CI) |
			Lower	Upper	
Planning CT					
GLCM3:Variance	0.012	9.58	1.643	55.862	0.894 (0.766–1.000)
ID:GlobalMedian	0.043	1.508	1.012	2.246	
CBCT1					
GLCM3:ClusterShade	0.022	2.778	1.158	6.661	0.918 (0.819–1.000)
ID:LocalEntropyMax	0.037	0	0	0.517	
SHAPE:Orientation	0.113	0.943	0.878	1.014	
CBCTmid					
GLCM3: InformationMeasureCorr2	0.049	1.066	1	1.135	0.697 (0.486–0.908)
CBCTlast					
GLCM3: InformationMeasureCorr2	0.029	1.102	1.01	1.202	0.764 (0.563–0.966)

CBCT1, the first CBCT during SBRT; CBCTmid, intermediate CBCT during SBRT; CBCTlast, last CBCT during SBRT.

[-B] = 1.060). The area under the curve was 0.918, and the 95% CI was 0.819–1.000. One radiomics feature (GLCM3: InformationMeasureCorr2) of CBCTmid was significantly correlated with disease progression. For each additional unit of GLCM3:InformationMeasureCorr2, the risk of progression increased by 6.6% (OR = Exp [B] = 1.066), and the area under the curve was 0.697 (95% CI: 0.486–0.908). One radiomics feature (GLCM3: Information Measure Corr2) of CBCTlast was significantly correlated with progression. With each unit increase in the GLCM3: Information Measure Corr2 radiomics feature, the risk of progression increased by 10.2%. The area under the curve was 0.764, and the 95% CI was 0.563–0.966. (Table 2).

The ROC curves of the prognostic model based on the planning CT radiomic features and that based on the radiomics features of the CBCTs plus planning CT (planning CT + CBCT1 + CBCTmid + CBCTlast) were compared. The ROC curves were used to evaluate the predictive ability of the models. The AUCs were 0.913 and 0.885, respectively. The results indicated that the model based on the planning CT had a similar prediction ability to the model based on the planning CT plus CBCT (Fig 2).

Correlation between radiomics features and lung injury

Two planning CT radiomics features (SHAPE: Mass and SHAPE: Orientation) were significantly correlated with lung injury. With each unit increase in radiomics feature SHAPE: Mass, the risk of lung injury increased by 32.456 times (OR = Exp [B] = 33.456). For each additional unit of SHAPE: Orientation, the risk of lung injury increased by 4.7% (OR = Exp [B] = 1.047). The area under the curve was 0.832, and the 95% CI was 0.621–1.000 (Table 3).

Two CBCT1 radiomics features (NGTDM25: Contras and SHAPE: Max3D Diameter) were correlated with lung

injury. The risk of lung injury increased by 0.1% (OR = Exp [B] = 1.001) for each additional unit of NGTDM25: Contras. The risk of lung injury increased by 3.094 times (OR = Exp [B] = 4.094) for each additional unit of SHAPE: Max3D Diameter. AUC was 0.87, and the 95% CI was 0.683–0.990. Two CBCTmid radiomics features (ID: 60Percentile and NGTDM25: Complexity) were correlated with lung injury. With each unit increase in radiomics feature (ID: 60Percentile), the risk of lung injury
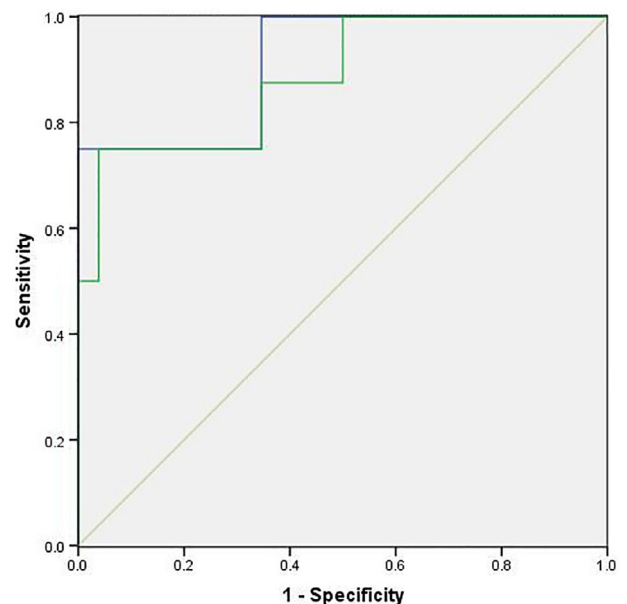

Figure 2 Receiver operating characteristic (ROC) curve for disease progression. The ROC curves of the prognostic models based on the planning CT radiomics features alone and on the radiomics features of the CBCTs and planning CT (CBCT1 + CBCTmid + CBCTlast + planning CT) were compared. The ROC curves were used to evaluate the prediction models, and the AUCs were 0.913 and 0.885, respectively. —— CT, ——CT + CBCTs, ——Reference line.

Table 3 The radiomic features correlated with lung injury

Radiomic features	*P*-value	Exp (B)	Exp (B) 95% CI		Logistic regression AUC (95%CI)
			Lower	Upper	
Planning CT					
SHAPE:Mass	0.011	33.456	2.257	496.017	0.832 (0.621–1.000)
SHAPE:Orientation	0.036	1.047	1.003	1.093	
CBCT1					
NGTDM25:Contrast	0.077	1.001	1	1.003	0.837 (0.683–0.990)
SHAPE:Max3DDiameter	0.008	4.094	1.438	11.659	
CBCTmid					
ID:60Percentile	0.074	1.197	0.983	1.457	0.861 (0.735–0.986)
NGTDM25:Complexity	0.065	1	1	1	
CBCTlast					
GLCM3:ClusterProminence	0.047	1.45	1.006	2.09	0.952 (0.885–1.000)
SHAPE:ConvexHullVolume	0.019	1.102	1.016	1.194	

CBCT1, the first CBCT during SBRT; CBCTmid, intermediate CBCT during SBRT; CBCTlast, last CBCT during SBRT.

increased by 19.7% (OR = Exp [B] = 1.197). The radiomics feature NGTDM25 Complexity showed a weak correlation with lung injury (OR = Exp [B] = 1.000). The area under the curve was 0.861 (95% CI: 0.735–0.986). Two CBCTlast radiomics features (GLCM3: ClusterProminence and SHAPE: ConvexHullVolume) were significantly correlated with lung injury. With each unit increase in the radiomics feature GLCM3: ClusterProminence, the risk of lung injury increased by 45% (OR = Exp [B] = 1.450). With each unit

increase in the radiomics feature SHAPE: ConvexHullVolume, the risk of lung injury increased by 10.2% (OR = Exp [B] = 1.102). The AUC was 0.952, and the 95% CI (0.885–1.000) (Table 3).

The ROC curves of the prediction models of lung injury based on planning CT radiomics features alone and on the radiomics features of CBCTs plus the planning CT (planning CT + CBCT1 + CBCTmid + CBCTlast) were compared. ROC curves were used to evaluate the models, and AUCs were 0.832 and 0.885, respectively (*P* = 0.367). When the sensitivity of the CBCTs plus the planning CT model and the planning CT model was constant (87.5%), the specificity of the CBCTs plus the planning CT model was 84.62%, the specificity of the planning CT model was 80.77%. The results indicated that the model based on CBCTs combined with planning CT might have a better prediction ability than the model based on the planning CT alone (Fig 3 and Table 4).
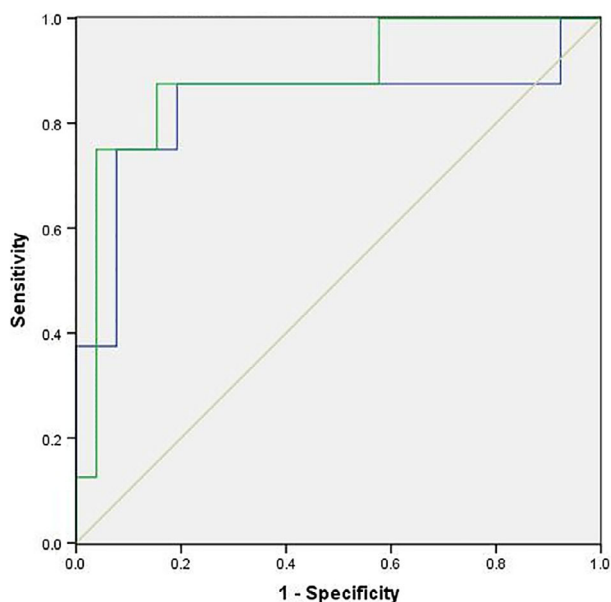

Figure 3 Receiver operating characteristic (ROC) curve for lung injury. The ROC curves of prediction models of lung injury based on planning CT radiomics features alone and on the radiomics features of the CBCTs plus planning CT (planning CT + CBCT1 + CBCTmid + CBCTlast) were compared. The ROC curves were used to evaluate the models, and the areas under the curve AUCs were 0.832 and 0.885, respectively. —— CT, —— CT + CBCTs, —— Reference line.

Discussion

With the development of lung cancer screening and radiotherapy techniques, more and more early-stage NSCLC patients will be diagnosed and treated with SBRT. Therefore, it becomes important to look for more features to predict or monitor treatment efficacy and/or toxicity. In this study, the predictive effect of a model that combined CBCT radiomics features with planning CT radiomics features for disease progression and radiation pneumonitis in stage I NSCLC patients treated with SBRT was explored. The results suggested that a model based on CBCT radiomics features combined with planning CT radiomics features might improve the prediction of lung toxicity after SBRT in comparison to a model based on pretreatment CT features alone.

Table 4 Receiver operating characteristic (ROC) curves analysis for lung injury of the planning CT model and the CBCTs plus planning CT model

Model	AUC	95% CI	*P*-value	Sensitivity	Specificity
Planning CT	0.832	0.664–0.938	<0.0001	87.5%	80.77%
CBCTs + Planning CT	0.885	0.728–0.968	0.0036	87.5%	84.62%

Previous studies found that changes in tumor density and volume obtained from CBCT images predicted treatment response to chemoradiation therapy in advanced NSCLC patients. A reduction in tumor volume on CBCT during definitive chemoradiotherapy correlated with improved disease control and overall survival of stage III–IV non-small cell lung cancer patients.[23–25] These studies have reported inconsistent time points, CBCT-measured tumor volumes and/or density changes associated with the clinical outcomes. To address this problem, in this study, the radiomics features of CBCTs acquired at three different time points (CBCT1, CBCTmid and CBCTlast) were explored. The results showed that the CBCT radiomics features were significantly correlated with PFS. However, the model that combined CBCT and planning CT radiomics features did not yield an improved prediction capacity. Previous studies have shown that the CBCT imaging features could assess response to treatment and serve as an early biomarker.[29,30] By summarizing previous research findings on NSCLC, we found that the radiomics features of CT and CBCT were interchangeable and that the radiomics features of the CBCT prior to the first fraction of treatment showed prognostic information for the overall survival of NSCLC patients acquired.[31] The radiomics features of CBCTs acquired early during a course of treatment may be associated with overall survival in locally advanced NSCLC.[32]

No studies have so far been performed to correlate lung injury with the CBCT radiomics features of NSCLC. In this study, the CBCT radiomics features were analyzed, and we found that the radiomics features were significantly correlated with lung injury after SBRT. More importantly, the model that combined CBCT and planning CT radiomics features might improve the prediction of lung toxicity after SBRT than the model based on pretreatment CT radiomics features alone. The CBCT imaging features of the parotid gland could predict chronic xerostomia better than the dose alone. Analyses of the CBCT images acquired for treatment positioning may provide an inexpensive monitoring system to support toxicity-reducing adaptive radiation therapy.[33]

Since the number of patients in our study was relatively small, and the good outcome of SBRT (low toxicity and progression), there were limited patients with lung injury (23.5%, *n* = 8) and disease progression (23.5%, *n* = 8). The AUC of CBCT plus planning CT model was 0.885 and the planning CT model was 0.832 based on the ROC curves with

prediction in lung injury models. Although it failed to obtain significant statistical difference, the specificity of CBCTs plus planning CT model was higher than the model with planning CT alone (84.62% and 80.77%) when the sensitivity was constant at 87.5%. There was a tendency that radiomics features of CBCT plus planning CT might improve the prediction in lung injury than the planning CT features alone.

There were several limitations in the study. First, the sample size was limited. Future studies with larger numbers of patients are necessary to validate our results. Second, CBCT radiomics features typically depend on reconstruction and scanning parameters.[34–37] The different slice thicknesses used in CT and CBCT reconstruction could influence the accuracy of the values, and the potentially limited soft-tissue contrast of CBCT compared with that of CT could lead to uncertainties.[38] Therefore, only CBCT images with a 3 mm slice thickness, which was identical to the slice thickness of the CT images, were used to ensure consistency throughout this study. Finally, although the image quality of CBCT is not as good as the diagnostic CT, the CBCT imaging quality might improve with the application of Monte Carlo-based scatter correction and other techniques[26,27] The advantage of CBCT is that it detects the changes inside the tumor in time during the treatment, which may be helpful to adjust the patient's adaptive treatment plan. It prompts us to further improve the CBCT image quality and proceed with subsequent studies to evaluate the value of the CBCT radiomics features.

In conclusion, our study suggested that CBCT imaging features could potentially be applied as imaging biomarkers in addition to CT features. Earlier and different information about a patient's prognosis are needed to explore individualized treatment options to prolong the survival of stage I NSCLC patients after SBRT.

In the prediction of PFS and lung toxicity in early-stage NSCLC patients treated with SBRT, CBCT radiomics could be another effective method. It is possible to use the radiomics features of CBCT images acquired at different time points to predict the clinical outcome and toxicity of stage I NSCLC patients treated with SBRT as early as possible.

Acknowledgments

the manuscript. RZ acquired the patient data. TYN, YDW, JHC and QTQ for physical technical support. LGX and QW edited and corrected the manuscript.

Disclosure

There were no potential conflicts of interest, including specific financial interests and relationships in our manuscript, and the authors have no conflicts of interest.

References

1 Guckenberger M, Klement RJ, Allgauer M *et al.* Applicability of the linear-quadratic formalism for modeling local tumor control probability in high dose per fraction stereotactic body radiotherapy for early stage non-small cell lung cancer. *Radiother Oncol* 2013; **109** (1): 13–20.

2 Navarria P, Ascolese AM, Mancosu P *et al.* Volumetric modulated arc therapy with flattening filter free (FFF) beams for stereotactic body radiation therapy (SBRT) in patients with medically inoperable early stage non small cell lung cancer (NSCLC). *Radiother Oncol* 2013; **107** (3): 414–8.

3 Lo S S, Fakiris A J, Chang E L *et al.* Stereotactic body radiation therapy: A novel treatment modality. *Nature* 2010; **7**: 44–54.

4 National Comprehensive Cancer Network. NCCN guidelines for non-small cell lung cancer (version4.2017), 2017. [Cited 26 Feb 2017.] Available from URL: http://www.nccn.org/professionals/physician_gls/f_guidelines.asp.

5 Chang JY, Senan S, Paul MA *et al.* Stereotactic ablative radiotherapy versus lobectomy for operable stage I non-small-cell lung cancer: A pooled analysis of two randomised trials. *Lancet Oncol* 2015; **16** (6): 630–7.

6 Palma DA, Senan S. Improving outcomes for high-risk patients with early-stage non-small-cell lung cancer: Insights from population-based data and the role of stereotactic ablative radiotherapy. *Clin Lung Cancer* 2013; **14** (1): 1–5.

7 Timmerman RD, Paulus R, Pass HI *et al.* Stereotactic body radiation therapy for operable early- stage lung cancer: Findings from the NRG Oncology RTOG 0618 trial. *JAMA Oncol* 2018; **4** (9): 1263–6.

8 Onishi H, Shirato H, Nagata Y *et al.* Stereotactic body radiotherapy (SBRT) for operable stage I non-small-cell lung cancer: Can SBRT be comparable to surgery? *Int J Radiat Oncol Biol Phys* 2011; **81** (5): 1352–8.

9 Louie AV, Rodrigues G, Hannouf M *et al.* Stereotactic body radiotherapy versus surgery for medically operable stage I non-small-cell lung cancer: A Markov model-based decision analysis. *Int J Radiat Oncol Biol Phys* 2011; **81** (4): 964–73.

10 Ball D, Mai GT, Vinod S *et al.* Stereotactic ablative radiotherapy versus standard radiotherapy in stage 1 non-small-cell lung cancer (TROG 09.02 CHISEL): A phase 3, open-label, randomised controlled trial. *Lancet Oncol* 2019; **20** (4): 494–503.

11 Lambin P, van Stiphout RG, Starmans MH *et al.* Predicting outcomes in radiation oncology–multifactorial decision support systems. *Nat Rev Clin Oncol* 2013; **10** (1): 27–40.

12 Lambin P, Roelofs E, Reymen B *et al.* Rapid learning health care in oncology - an approach towards decision support systems enabling customised radiotherapy. *Radiother Oncol* 2013; **109** (1): 159–64.

13 Lambin P, Zindler J, Vanneste BG *et al.* Decision support systems for personalized and participative radiation oncology. *Adv Drug Deliv Rev* 2017; **109**: 131–53.

14 Carvalho S, Leijenaar RT, Velazquez ER *et al.* Prognostic value of metabolic metrics extracted from baseline positron emission tomography images in non-small cell lung cancer. *Acta Oncol* 2013; **52** (7): 1398–404.

15 Fried DV, Tucker SL, Zhou S *et al.* Prognostic value and reproducibility of pretreatment CT texture features in stage III non-small cell lung cancer. *Int J Radiat Oncol Biol Phys* 2014; **90** (4): 834–42.

16 Ganeshan B, Panayiotou E, Burnand K, Dizdarevic S, Miles K. Tumour heterogeneity in non-small cell lung carcinoma assessed by CT texture analysis: A potential marker of survival. *Eur Radiol* 2012; **22**: 796–802.

17 Coroller TP, Grossmann P, Hou Y *et al.* CT-based radiomics signature predicts distant metastasis in lung adenocarcinoma. *Radiother Oncol* 2015; **114** (3): 345–50.

18 Lambin P, Rios-Velazquez E, Leijenaar R *et al.* Radiomics: Extracting more information from medical images using advanced feature analysis. *Eur J Cancer* 2012; **48** (4): 441–6.

19 Kumar V, Gu Y, Basu S *et al.* Radiomics: The process and the challenges. *Magn Reson Imaging* 2012; **30** (9): 1234–48.

20 Gillies RJ, Kinahan PE, Hricak H. Radiomics: Images are more than pictures,they are data. *Radiology* 2016; **278**: 563–77.

21 Jaffray DA, Siewerdsen JH, Wong JW, Martinez AA. Flat-panel cone-beam CT for image-guided radiation therapy. *Int J Radiat Oncology Biol Psychol* 2002; **53**: 1337–49.

22 Brink C, Bernchou U, Bertelsen A, Hansen O, Schytte T, Bentzen SM. Locoregional control of non-small cell lung cancer in relation to automated early assessment of tumor regression on cone beam computed tomography. *Int J Radiat Oncol Biol Phys* 2014; **89**: 916–23.

23 Wen Q, Zhu J, Meng X *et al.* The value of CBCT-based tumor density and volume variations in prediction of early response to chemoradiation therapy in advanced NSCLC. *Sci Rep* 2017; **7** (1): 14650.

24 Wald P, Mo X, Barney C *et al.* Prognostic value of primary tumor volume changes on kV-CBCT during definitive chemoradiotherapy for stage III non-small cell lung cancer. *J Thorac Oncol* 2017; **12** (12): 1779–87.

25 Jabbour SK, Kim S, Haider SA *et al.* Reduction in tumor volume by cone beam computed tomography predicts overall survival in non-small cell lung cancer treated with chemoradiation therapy. *Int J Radiat Oncol Biol Phys* 2015; **92** (3): 627–33.

26 Westberg J, Jensen HR, Bertelsen A, Brink C. Reduction of Cone-Beam CT scan time without compromising the accuracy of the image registration in IGRT. *Acta Oncol* 2010; **49**: 225–9.

27 Xiance J, Weigang H, Haijiao S *et al.* CBCT-based volumetric and dosimetric variation evaluation of volumetric modulated arc radiotherapy in the treatment of nasopharyngeal cancer patients. *Radiat Oncol* 2013; **8**: 279.

28 DeLong ER, DeLong DM, Clarke-Pearson DL. Comparing the areas under two or more correlated receiver operating characteristic curves: A nonparametric approach. *Biometrics* 1988; **44** (3): 837–45.

29 Bertelsen A, Schytte T, Bentzen SM, Hansen O, Nielsen M, Brink C. Radiation dose response of normal lung assessed by cone beam CT - A potential tool for biologically adaptive radiation therapy. *Radiother Oncol* 2011; **100**: 351–5.

30 Bernchou U, Hansen O, Schytte T *et al.* Prediction of lung density changes after radiotherapy by cone beam computed tomography response markers and pre-treatment factors for non-small cell lung cancer patients. *Radiother Oncol* 2015; **117** (1): 17–22.

31 van Timmeren JE, Leijenaar RTH, van Elmpt W *et al.* Survival prediction of non-small cell lung cancer patients using radiomics analyses of cone-beam CT images. *Radiother Oncol* 2017; **123** (3): 363–9.

32 Shi L, Rong Y, Daly M *et al.* Cone-beam computed tomography-based delta-radiomics for early response assessment in radiotherapy for locally advanced lung cancer. *Phys Med Biol* 2020; **65**: 015009.

33 Rosen BS, Hawkins PG, Polan DF *et al.* Early changes in serial CBCT-measured parotid gland biomarkers predict chronic xerostomia after head and neck radiation therapy. *Int J Radiat Oncol Biol Phys* 2018; **102** (4): 1319–29.

34 Aerts HJ, Velazquez ER, Leijenaar RT *et al.* Decoding tumour phenotype by noninvasive imaging using a quantitative radiomics approach. *Nat Commun* 2014; **5**: 4006.

35 Mackin D, Fave X, Zhang L *et al.* Measuring computed tomography scanner variability of radiomics features. *Invest Radiol* 2015; **50** (11): 757–65.

36 Balagurunathan Y, Gu Y, Wang H *et al.* Reproducibility and prognosis of quantitative features extracted from CT images. *Transl Oncol* 2014; **7** (1): 72–87.

37 Balagurunathan Y, Kumar V, Gu Y *et al.* Test-retest reproducibility analysis of lung CT image features. *J Digit Imaging* 2014; **27** (6): 805–23.

38 Rosario M, Alba F, Francesco R *et al.* Cone-beam computed tomography in lung stereotactic ablative radiation therapy: Predictive parameters of early response. *Br J Radiol* 2016; **89**: 0146.